Chinese Chemical Letters 32 (2021) 2637–2647

Contents lists available at ScienceDirect

Chinese Chemical Letters

journal homepage: www.elsevier.com/locate/cclet

Review

Selective adsorption of phosphate in water using lanthanum-based nanomaterials: A critical review

Mamitiana Roger Razanajatovo[a], Wenyan Gao[a], Yaran Song[a,*], Xuan Zhao[a], Qina Sun[a], Qingrui Zhang[a,b,*]

[a] Hebei Key Laboratory of Heavy Metal Deep-Remediation in Water and Resource Reuse, and the Laboratory of Applied Chemistry, Yanshan University, Qinhuangdao 066004, China
[b] State Key Laboratory of Metastable Materials Science and Technology, Yanshan University, Qinhuangdao 066004, China

ARTICLE INFO

Article history:
Received 17 November 2020
Received in revised form 16 December 2020
Accepted 12 January 2021
Available online 2 February 2021

Keywords:
Lanthanum-nanomaterials
Synthesis
Phosphate
Adsorption mechanism
Regeneration
Application

ABSTRACT

In recent years, lanthanum-based nanomaterials (La-NMs) are selected as an efficient nano-adsorbent for phosphate removal because La^{3+} has a strong affinity with oxygen-donor atoms from phosphate. Additionally, there are a broad interest and literature base for the effect of different synthesis optimization and environmental parameters on the adsorption performance of La-NMs. A considerable amount of research has also investigated the regeneration and application of La-NMs to real wastewater in a laboratory scale. Based on the literature survey, it was found that La-NMs are often produced *via* co-precipitation and hydrothermal methods. Moreover, phosphate's adsorption process and behavior onto La-NMs are described well with the *pseudo*-second-order model and Langmuir model. The interaction mechanism between phosphate and La-NMs are dominated by ligand exchange, surface complexation and electrostatic attraction. Furthermore, phosphate could easily desorb from La-NMs due to the weak H-bonding interaction between phosphate and the H-bond acceptor groups on the surface of La-NMs. Despite the wealth of literature available in this area, there is a lack of systematic review to evaluate the gaps in the use of La-NMs to eliminate phosphate in water. In this review, we mainly summarize and discuss the role and the effect of the synthesis techniques on the physicochemical properties and the adsorption behavior of La-NMs. The possible adsorption mechanism, regeneration efficiency, and the application of La-NMs to the real environmental samples are also presented and highlighted.

1. Introduction

Water scarcity, poor water quality, and sustainable water resource management are significant challenges worldwide [1]. Moreover, due to the rapid population growth, advances in industrial and agriculture, the world faces a major problem of coping with water pollution [2,3]. In addition to that, the excessive discharge of phosphorus in the aquatic ecosystem has gained significant interest from past decades since it threatens the aquatic ecosystem and endangers the drinking water supply [4,5].

Besides, in recent years, various study fields have shown great interest in the application of nanotechnologies, such as in the biomedicine field [6,7], the catalysis field [8], and the environmental remediation field [9,10]. For the environmental remediation area, metal nanomaterials have attracted more and more attention for phosphate removal from water due to their high

* Corresponding authors at: Hebei Key Laboratory of Heavy Metal Deep-Remediation in Water and Resource Reuse, and the Laboratory of Applied Chemistry, Yanshan University, Qinhuangdao 066004, China.
E-mail addresses: songyr@ysu.edu.cn (Y. Song), zhangqr@ysu.edu.cn (Q. Zhang).

https://doi.org/10.1016/j.cclet.2021.01.046
1001-8417/

surface to volume ratio, stable optical properties, and good biocompatibility [11]. Among metal nanomaterials, rare earth metal lanthanum (La) is considered as an efficient nano-adsorbent to remove phosphate in water and wastewater because of its efficient antibacterial agent [12], environmentally friendly material, and relatively inexpensive rare earth element [13]. Meanwhile, La naturally has a strong affinity with phosphate, and La^{3+} ions can attract oxygen-donor atoms from phosphate through the anion-ligand exchange process.

Additionally, La could form a complex La-phosphate ($LaPO_4$) even at phosphate trace levels [14–16]. However, La nanoparticles (La-NPs) are susceptible to aggregation because of its high surface energy, van der Waals forces interaction, *etc*. This aggregation behavior results in a decrease of La-NPs pressure and mechanical strength [13], making it difficult to separate, recover, and even be useless to the real environment [17,18]. Thus, to overcome this issue, extensive attention has been directed to developing various carrier materials to embed La nanoparticles.

Research on the development of La-based nanomaterials (La-NMs) to adsorb phosphate in water is growing promptly, which is reflected by the annual increase of research articles published in the last ten years (Fig. 1). To date, several review articles have summarized the potential of La-NMs to remove phosphate. For example, Copetti *et al.* was resumed and discussed the application of modified bentonite (Phoslock®) to control water eutrophication [19]. Recently, Wu *et al.* was also provided a detailed overview of phosphate-selective adsorbents developments and explained the recent advanced approaches achieving selective phosphate removal from water and wastewater [20]. Moreover, Zhi *et al.* has reported the application of lanthanum materials (LM) for phosphate removal in laboratory studies and field-scale applications. They have also discussed the role of environmental factors and the potential impacts of LM on ecological systems [21].

However, based on our knowledge, there is a lack of a systematic review available, which notably provides comprehensive information concerning the role and effect of various synthesis methods on La-NMs properties, and on the adsorption behaviors of La-NMs toward phosphate. For this reason, the ultimate goals of this present review are to: (1) Emphasize the role and effect of various synthesis procedure on the structure, properties, and adsorption performance of La-NMs; (2) discuss the potentiality of various La-NMs to remove phosphate in aqueous solution and real wastewater; (3) elucidate the evidence of selective removal of phosphate by La-NMs and the possible interaction mechanisms; (4) highlight the regeneration and the application of these materials to real environmental sample. Finally, we analyze the future development of La-NMs.

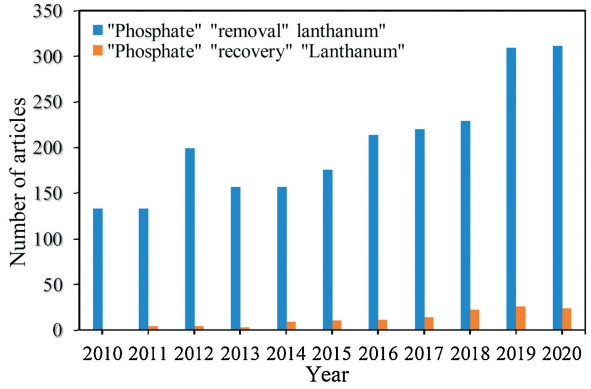

Fig. 1. Evolution on the number of published papers between 2010 and 2020 with the keywords: "phosphate", "removal", and "lanthanum"; "phosphate" "recovery" "lanthanum" (sources: Web of Science and Scopus).

2. Synthesis methods and physicochemical characterization of La-NMs

2.1. Synthesis process of La-NMs

Extensive data shows that the shape and the size of La-NMs are the parameters that may affect phosphate adsorption efficiency [22,23]. Several synthetic strategies have been developed to obtain La-NMs with narrow size distribution, uniform shape, and unique functionalities in the past few years [24,25]. Fig. 2 illustrates the synthesis techniques of La-NMs. Numerous available literature shows that among the La-NMs synthesis methods, co-precipitation and hydrothermal are the synthesis protocols widely used (Table S1 in Supporting information). The main reason for this is the low-cost, high efficiency, and simple operation of these synthesis methods [26–29]. The following paragraph discusses the synthesis process, the advantages and disadvantages of the co-precipitation and hydrothermal synthesis techniques.

The chemical co-precipitation method is the simplest and most efficient for preparing La-NMs. Based on our literature survey, La-NMs co-precipitation process could be summarized in three steps: (1) The preparation of La and the host materials solution in the liquid phase with the chemical composition; (2) the addition of a precipitation agent such as NaOH, urea, which may vary the sizes of the nanoparticles; and (3) precipitate separation following by a thermal treatment that influences the crystallinity, morphology, and structure of the La-NMs [30–32]. Various La-NMs such as single lanthanum oxide and hydroxide [18,31,33], lanthanum-chitosan nanocomposite (La-CTS) [34], $La(OH)_3$-modified magnetic cobalt ferric ($CoFe_2O_4$) nanocomposites (La-CF) [17], magnetite ferihydric lanthanum (Mag@Fh-La) [35], lanthanum-incorporated porous zeolite (La-Z) [36], novel talc encapsulated lanthanum alginate hydrogel (TAL beads) [37], *etc*. have been produced through co-precipitation method. Based on the literature, we found that the co-precipitation technique is appropriate for synthesizing magnetite-La-NMs by a stoichiometric mixture of ferrous and ferric salts in an aqueous medium [38,39]. On the other hand, the precipitation process is complex since numerous reactions such as growth, nucleation, and aggregation could be occurring simultaneously [40]. Besides, the uncontrollable nanoparticle size, the non-uniform shape, and low crystalline nature of the products (Figs. 3a and b) are the main disadvantages of this synthesis route [41]. Thus, hydrothermal synthesis is adopted to overcome these issues.

In general, the hydrothermal synthesis conduct in Teflon-lined stainless steel autoclave under controlled pressure and/or temperature [42]. The synthesis temperature often depends on the solvent used in the process. The temperature is generally elevated to above the solvent's boiling point to reach pressure vapor saturation [43]. The hydrothermal protocol is among the most convenient and practical techniques for La-NMs fabrication as it enables the avoidance of special instruments and complicated processes [44]. In addition to that, the main advantages of this synthesis route are that it provides an easy way to produce excellent and high crystallinity La-NMs, and controllable shape and size of the desired La-NMs products [45] (Figs. 3c and d). Numerous La-NMs such as zeolite coated lanthanum hydroxide nanocomposite (La-ZFA) [46], lanthanum-incorporated porous zeolite (La-Z) [36], magnetic Fe_3O_4 core-shell lanthanum (MFC@$La(OH)_3$) [47], periclase lanthanum nanocomposite (PC@La) [44], magnetic adsorbent $NaLa(CO_3)_2/Fe_3O_4$ [48], 3D rice-like lanthanum-doped La@MgAl nanocomposites [49], nanosized lanthanum hydrous doped on magnetic graphene nanocomposite (MG@La) [50], *etc*. have been made by using the hydrothermal synthesis. In contrast, the high cost of the autoclave, uncontrolled safety issues during the reaction process, and the impossibility of observing the reaction

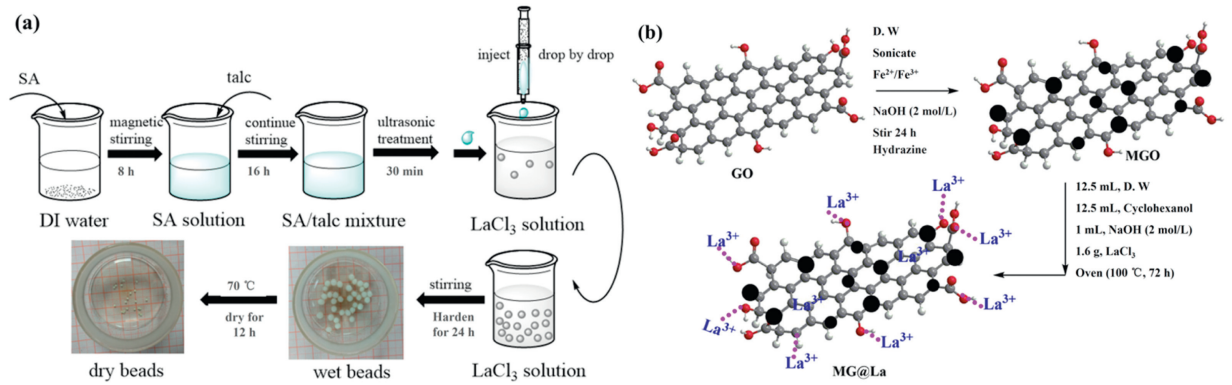

Fig. 2. Schematic illustration of La-NMs synthesis process *via* precipitation (a) and *via* hydrothermal method (b). (a) Reproduced with permission [37]. Copyright 2020, Elsevier. (b) Reproduced with permission [50]. Copyright 2017, Elsevier.

process are considered the main disadvantages of hydrothermal synthesis [51].

The lanthanum phase loaded on the host materials is varied among the different synthesis methods, resulting in the distinct adsorption behavior and mechanism toward phosphate [52,53]. The characterizations and properties of the hybrid La-NMs are discussed in the subsequent section.

2.2. Characterization and surface properties of La-NMs

The surface characterization and the structure of bonds that existed in the surface of La-NMs are essentially analytical tools to confirm the successfully loaded of La ions on the surface or in the pore of the carrier materials. And also useful to understand the possible interaction mechanism between phosphate and La-NMs. The use of scanning electron microscopy (SEM), transmission electron microscopy (TEM), and triple-point-nitrogen Brunuaer-Emmett-Teller (BET) could achieve the characterization of the surface morphology, size, and surface area of La-NMs. Besides, X-ray diffraction spectrometer (XRD), Fourier transform IR spectroscopy (FTIR), X-ray Photoelectron Spectroscopy (XPS), and zeta potential could determine and analyze the crystal structure, the existence of lanthanum on the host material, the structural bonds in La incorporated adsorbent, and the isoelectric charge distribution of La-NMs.

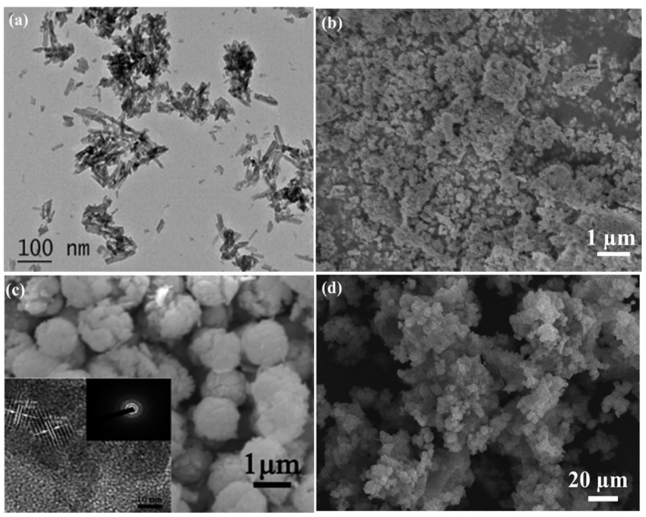

Fig. 3. SEM and TEM images of La-NMs products prepared by precipitation (a and b) and hydrothermal (c and d). (a) TEM image of Lanthanum oxide. Reproduced with permission [53]. Copyright 2019, Elsevier. (b) FESEM of Fe-Mg-La triple-metal composite. Reproduced with permission [41]. Copyright 2015, Elsevier. (c) SEM of spherical La_2O_3. Reproduced with permission [45]. Copyright 2017, The Royal Society of Chemistry. (d) SEM image of lanthanum hydroxide loaded on molecular sieve. Reproduced with permission [56]. Copyright 2018, Elsevier.

After a successful synthesis process, the structure and surface properties of the synthesized La-NMs are significantly different compared to the pure host materials (Fig. 4). Table S1 illustrates the difference in the properties between the pure carrier adsorbent and the synthesized La-NMs. For the La-NMs prepared by the co-precipitation method, the product's surface properties are affected by the synthesis optimization, such as synthesis time. Recent work demonstrated that the specific surface area of lanthanum carbonate grafted micro-fibrous composite (LC-MC) is significantly enhanced by increasing the synthesis time. The longer synthesis time allowed La and urea to have sufficient time for interaction [24]. On the contrary, He *et al.* showed that the longer incorporation of La into the activated zeolite was decreased the specific surface area, total pore volume, and the average pore diameter of the synthesized lanthanum-incorporated porous zeolite (La-Z). This was due to the lanthanum oxide blocked zeolite mesopores and aggregated on the surface [36].

For the La-NMs prepared by the hydrothermal synthesis, the carrier materials' surface element content was dropped after a successful hydrothermal reaction. For example, the sodium content in lanthanum zeolite (La-ZFA) was reduced due to the partial exchange of sodium ions on the zeolite surface by the La ions hydroxide [54]. Moreover, Qiu *et al.* observed that the number of grooves on the La incorporated wheat straw was increased apparently after the synthesis reaction. Additionally, the surface morphology of La-wheat straw became much coarser [13]. This is the phenomenon that explains the increase of adsorption sites on the novel synthesized La-NMs. Zhang *et al.* also carried out conceptually similar work. The authors found that compared to the new D201, the surface area of the La-D201 was enlarged two times. This finding arose from the fact that the uniformly immobilization and dispersion of La nanoparticles inside the networking pores of D201 [55]. Therefore, the distinct carrier materials for La and the synthesis process would make a significant difference in phosphate removal capacity, La usage efficiency, and the stability of La on the support materials.

The lanthanum species loaded on the host materials and the synthesis method process may also change La-NMs surface chemistry's nature. The surface chemistry of La-NMs was determined by the number and the nature of surface functional groups on the La-NMs surface. The type of the functional groups on La-NMs could predict its phosphate selectivity. Based on our survey, oxygen-containing functional groups (—OH and —COOH) [23,56–58] and nitrogen-containing functional groups (—NH_2 and

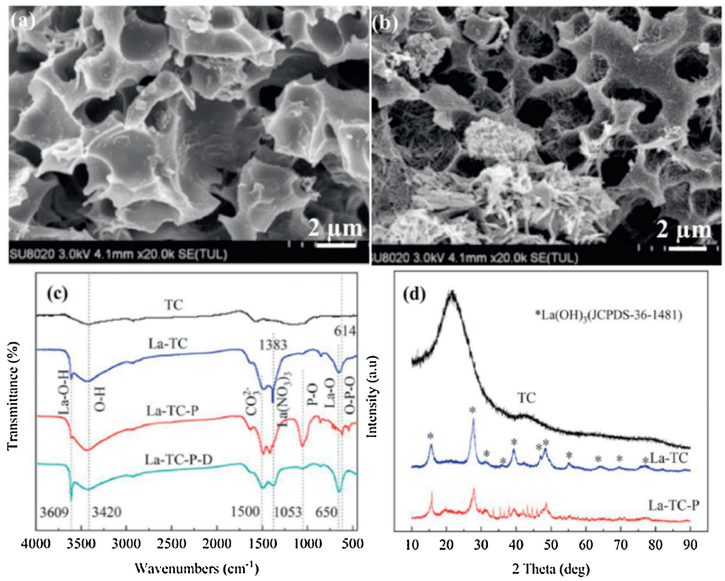

Fig. 4. The structure and surface properties of carrier materials before and after La coated: SEM of pristine carrier materials (a), SEM of synthesized La-NMs (b), FTIR spectra of La-NMs adsorbent before and after synthesis process (c), XRD spectra of La-NMs adsorbent before and synthesis process (d). Reproduced with permission [30]. Copyright 2020, Elsevier.

—NH) are among the most common functional groups on La-NMs [59,60]. These surface functional groups are found to contribute widely to phosphate adsorption because these two surface functional groups can serve as H-bond accepting sites, which can form H-bonds with the protonated phosphate anions (H_2PO_4, HPO_4^{2-}). For example, the FTIR analysis showed that a sharp peak at ~3450 cm^{-1} was appeared after the synthesis process, indicating the stretching vibrations of hydroxyl groups on novel lanthanum doped biochars derived from lignocellulosic wastes adsorbent [57], and Liu *et al.* found that the vibration of C—O located at 1092 cm^{-1}, which was assigned to the —COOH on lignin-derived porous carbon loaded with $La(OH)_3$ nanorods [23]. The XPS analysis of lanthanum hydroxides modified poly(epichlorohydrin)-ethylenediamine composites after precipitation synthesis showed that two peaks at 402.4 and 399.6 eV, which were assigned to the $—N^+(CH_3)_3$ and unreacted $—NH_2$ functional group on the poly (epichlorohydrin)-ethylenediamine (PEE). This indicated that the loaded of lanthanum on the PEE did not affect the large number of quaternary ammonium groups on the PEE matrix [60]. The detailed role of La-NMs surface functional groups is summarized in Section 3.5. The adsorption behavior, performance, and mechanism of various La-NMs prepared by various synthesis methods are discussed in the subsequent section.

3. Application of La-NMs in phosphate removal

This review covers up the thorough literature of the last ten years (2010–2020) undertaking the use of various La-NMs for the uptake of phosphate from water and wastewater. Table S2 (Supporting information) summarizes the maximum adsorption capacity and equilibrium time of different category La-adsorbents under different environmental conditions.

3.1. Single La and La-metal-based adsorbent

Among the rare earth elements, La nanoparticles are considered an effective adsorbent to eliminate phosphate from water due to lanthanum's strong affinity with phosphate through the anion-ligand exchange process between La^{3+} ions and oxygen-donor atoms from phosphate [55,61]. Enormous amounts of work have investigated the efficiency of the synthesized single lanthanum hydroxide (LHs), lanthanum oxide (LO), and lanthanum carbonate (LC) to remove phosphate in water [18,22,25,28,62–64].

It has experimentally demonstrated that La species are an important factor that could expand the adsorption capacity. To our knowledge, there is a lack of clarity due to the limited studies on the comparison of the adsorption behavior of different La species toward phosphate. Moreover, phosphate and fluoride are both anions; thus, in the case of fluoride, previous study indicated that the sorption capacity of three species lanthanum (LH, LO, and LC) toward fluoride followed the order of LO > LC > LH [53]. In the present study, we compare phosphate's effective removal by distinct La species according to several available literatures. Based on our survey, we find that single lanthanum hydroxide had the potential to uptake phosphate anions. Xie *et al.* observed that the maximum adsorption capacity of LHs (107.53 mg/g) was higher than that of LO (46.95 mg/g) [18,33]. The different sorption capacity among the La species is due to the different binding mechanism [53]. Various interaction mechanisms between La ions and phosphate ions are discussed in the subsequent paragraph.

The kinetics process of phosphate adsorbed to La nanoparticles firstly governed by the external surface adsorption, followed by the gradual adsorption, and finally reached the adsorption equilibrium [22,25,63]. Based on the *pseudo*-second-order model's best fit, the chemisorption process was dominated during the phosphate uptake by the LHs, LO, and LC nanoparticles [18,22,64]. Moreover, the adsorption behavior of phosphate onto La nanoparticles could be described by the monolayer homogeneous and multilayer heterogeneous, which is according to the best fitted of Langmuir and Freundlich models [28].

Many studies recently demonstrated that phosphate ion species are also an essential factor affecting the adsorption process under various pH. Fang *et al.* discovered that the phosphate adsorption by lanthanum hydroxide nanorods was gradually decreased from 6.45 mmol/L to 1.5 mmol/g, with the pH increasing from 4 to 10 [28]. This could in part be explained by the release of hydroxyl anions (OH^-) from lanthanum hydroxide at alkaline pH, which competes for the adsorption active sites with phosphate anions. Furthermore, under high pH conditions, the OH^- on $La(OH)_3$

probably exchanges with PO_4^{3-}, HPO_4^{2-}, and $H_2PO_4^-$ which was rapidly reduced the binding of phosphate on La-NMs [18]. On the contrary, at the acidic conditions, phosphate's adsorption capacity on $La(OH)_3$ nanoparticles was increased sharply. This result was due to the fact that at low pH, more H^+ were involved and attached with $La(OH)_3$ to attract the negatively charged ions of PO_4^{3-}, HPO_4^{2-}, and $H_2PO_4^-$. Thus, the main adsorption mechanisms at the acidic conditions were the collaboration of electrostatic reaction and ligand exchange [63].

Several studies have also revealed that coexisting anions (NO_3^-, SO_4^{2-}, and Cl^-) had an insignificant effect on phosphate's adsorption process onto single La nanoparticles. The highly selective phosphate adsorption under various coexisting anions by La-nanoparticles could be explained by several reasons, in which the dominance of the ligand exchange mechanism; the $LaPO_4$ crystallized along with the (110) plane of $La(OH)_3$ and ultimately grow of $LaPO_4$ on the surface of the La-nanoparticles [22,63]. Although La-nanoparticles can be used as an efficient adsorbent to sequester phosphate in water, but these materials are difficult to recover and separate from water due to the high aggregation behavior. This may result in the limits of their application [55]. Thus, to overcome this challenge, La species are incorporated onto various carrier materials, such as metal oxide support.

Nanosized metal (hydro)oxides such as hydrated ferric oxide and hydrous zirconium oxide have extensively developed due to their large specific surface areas and abundant hydroxyl groups on their surface active sites [65,66]. Thus, compared to the single La adsorbent, La coated on the multi-metal hydro(oxide) could potentially remove phosphate from water. The interaction mechanisms between La-metal-based nanomaterials and phosphate are the combination of ligand exchange, inner-sphere complexation, and electrostatic interaction mechanisms (Fig. 5). Moreover, due to the paramagnetic of La-metal adsorbent, especially La-coated on Fe_3O_4 nanoparticles, they could be recovered easily by applying magnetic separation [39].

Several studies have explored the use of La-metal hydro(oxide) adsorbents as tools to remove phosphate. In recent years, numerous studies have been investigated the potential of Lanthanum/aluminum hydroxide [67], Fe-La composite [68], Fe-Mg-La triple-metal [41], Mg-Al-La ternary hydroxide zeolite [69], Mg-La bimetal oxide nanocomposite [42], La-Zr-Zn ternary oxide [70], 3D rice like lanthanum doped La@MgAl nanocomposites [49], and $MgFe_2O_4$-biochar based lanthanum alginate beads [71] to remove phosphate in water. Wang *et al.* showed that the phosphate removal by Fe-La adsorbent was increased with increasing the solution pH from 3.8 to 6.2, and the maximum sorption efficiency was reached 90.6% at pH 3.2 [68]. It can be argued that this is because of the electrostatic attraction between $H_2PO_4^-$ and the protonation of the La-metal adsorbent. On the other hand, Shi *et al.* found that phosphate's adsorption on Mg-Al-La ternary hydroxide zeolite was declined at pH 3 and 11 [69]. There are several explanations for this, in which: (1) the protonation or deprotonation of La-metal surface groups [69]; (2) the formation of inner-sphere complexation by the exchange of —OH from La—OH with phosphate [67]; (3) and the leaching of the metal ions at alkaline pH [70]. Xu *et al.* elucidated that the maximum concentration released of Al^{3+} and La^{3+} was 0.078 mg/L and 0.077 mg/L at pH range from 7.0 to 9.0 [67]. This finding allows us to understand the ecological risk of La-NMs, which should consider when doing research about the application of La-NMs.

The adsorbent dose and the coexisting anions in the solution also had an important role in removing phosphate by La-metal-based adsorbents, which was demonstrated by recent studies [68,72]. The removal rate of phosphate was decreased with further increasing Fe-La composite dose. A plausible and useful theory behind this phenomenon is the adsorbent aggregation, which was limited the available activate sites [68]. Moreover, HCO_3^- and F^- could highly compete for sorption sites with phosphate by forming the inner-sphere complexes. A direct consequence of this competition was the decrease in phosphate uptake. Additionally, SO_4^{2-} also had a significant effect on the non-specific adsorption

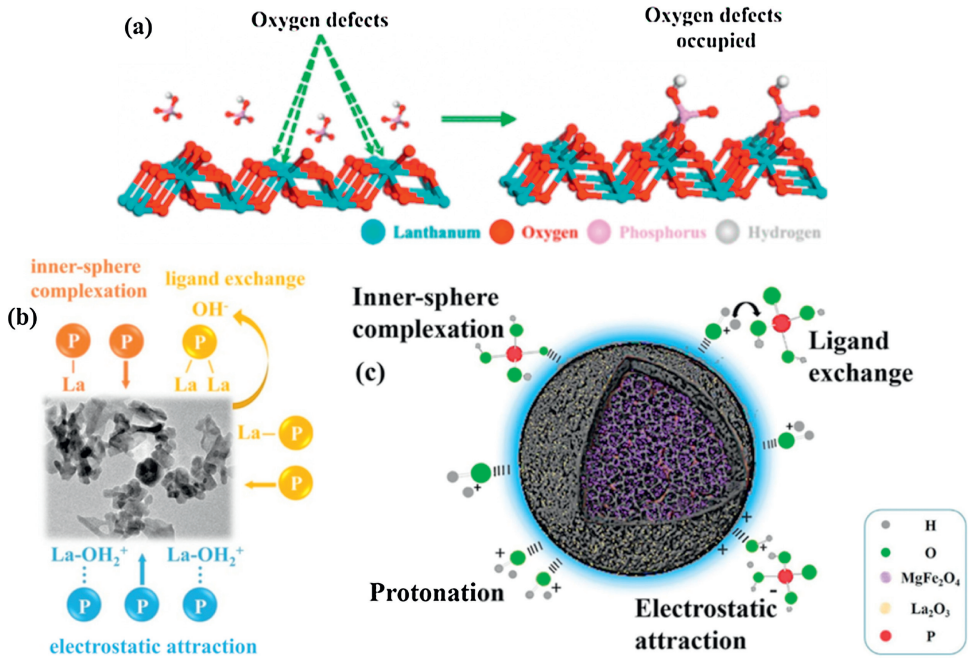

Fig. 5. Schematic illustration of adsorption mechanisms of phosphate by La-metal-based adsorbents. (a) Phosphate adsorption mechanisms onto Lanthanum/Aluminum—hydroxide composite. Copied with permission [67]. Copyright 2017, American Chemical Society. (b) Phosphate adsorption mechanisms onto $La(OH)_3$ modified magnetic cobalt ferrite ($CoFe_2O_4$) nanocomposites. Copied with permission [17]. Copyright 2020, Elsevier. (c) Phosphate adsorption mechanisms on $MgFe_2O_4$-biochar based lanthanum alginate beads. Reproduced with permission [71]. Copyright 2020, Elsevier.

process of phosphate by La-metal adsorbent, which was caused by electrostatic interaction of La-metal with higher charge density anions SO_4^{2-} [72].

Most of the La-metal-based adsorbent experimental data were fitted well with the Langmuir model, indicating a monolayer phosphate adsorption on this La-NMs category. Moreover, needle-like Mg-La bimetal oxide nanocomposites (PC@La) could sorb 107.34 mg/g of phosphate, and the isotherm data fitted well with the sips model [44]. The sips model's best fit emphasizes the interaction behavior between PC@La and phosphate are heterogeneous surface exerted multilayer interaction. Such La-metal based adsorbents are only feasible for the treatment of single target pollutant [73].

Phosphate ions interact with La-metal through different mechanisms. Several studies elucidated that ligand exchange is generally considered as the primary mechanism of phosphate affinity to La-metal-based adsorbent, which could be confirmed by the pH change after the adsorption process [44,72,73]. The possible interactions mechanism of phosphate adsorption by La-metal adsorbent can be expressed below (Eqs. 1–3):
Ligand exchange

$$\text{M-OH} + H_2PO_4^- \leftrightarrow \text{M-}H_2PO_4 + OH^- \quad (1)$$

Electrostatic attraction

$$\text{M-OH} + H_2O \leftrightarrow \text{M-}OH_2^+ + OH^- \quad (2)$$

$$\text{M-}OH_2^+ + H_2PO_4^- \leftrightarrow (\text{M-}OH_2^+)(H_2PO_4^-) \quad (3)$$

The removal of phosphate by La-metal-based adsorbents is very efficient. But the application of La-metal-based adsorbent is limited due to the poor mechanical strength and the high dissolution of this La-NMs category under extreme acidic/alkaline conditions. Moreover, except for iron-based host materials, most of La-metal based adsorbents are difficult to separate from water. Thus, researchers use other host materials such as natural minerals, carbon, biomaterial, polymers, to carry La ions.

3.2. La-natural mineral-based adsorbent

According to our literature survey, research focused on the phosphate uptake by La incorporated on natural mineral is more than La coated on the other support materials. This is because of the low cost, the simple operation, and the efficiency in pollution control of natural mineral materials. Natural mineral classifies as a natural compound are formed under the geological process, with a relatively fixed chemical composition including zeolite [36,74–78], clay [79–81], porous silica (SiO_2) [82–86] and other minerals [16,87–90].

For hybrid La-zeolite, the maximum adsorption capacity of phosphate on La/Al-ZA and lanthanum zeolite (La-ZFA) was 2.429 mg/g and 71.94 mg/g, respectively [46,54]. Extensive research has also carried out using SiO_2 decorated La for phosphate removal due to its low toxicity, structural stability, and SiO_2 support materials' chemical resistance. For example, phosphate's maximum sorption capacity by free-standing large-mesoporous silica films decorated with lanthanum (La-MSF) was 52.7 mg/g. Apart from La-MSF, the adsorption capacity of phosphate onto lanthanum(III)-coordinated diamino-functionalized 3D hybrid mesoporous silicates material (La-NN-M41) was increased rapidly and achieved 92.8% with a short time [84,91].

The temperature has an important role in the adsorption process of phosphate to La-natural mineral materials. Moreover, the temperature effect is varied among the category of natural mineral host materials. The phosphate's adsorption on La-zeolite (La-Z) was increased from 57.7 mg/g to 63.9 mg/g, with increasing the temperature from 25 °C to 60 °C [92]. This phenomenon can be explained by the greater mobility of phosphate ions in solution at a higher temperature, which increases the probability of collision between adsorption sites and phosphates ions [34]. On the other hand, the maximum adsorption capacity of phosphate onto La-NN-M41 was 54.3, 51.8, and 50.3 mg/g at 25, 35, and 45 °C, respectively [91]. This finding demonstrated that phosphate's adsorption behavior was exothermic, indicating that both physical and chemical interactions occurred in the adsorption process.

The adsorption behavior of La-natural mineral adsorbent varies among the solution pH, coexisting anions, and host natural mineral category. The sorption of phosphate by La-zeolite was significantly reduced with increasing pH from 2.5 to 10.5 [36,46,54]. Zhang *et al.* found that phosphate's adsorption capacity on La-NN-M41 was dropped at alkaline conditions due to the electrostatic repulsion between the deprotonated surface and highly charged phosphate anions. In comparison, the sorption amount of phosphate on La-NN-M41 was increased to 41.9 mg/g at pH 3. Moreover, La-NM-M41 still exhibited relatively high adsorption between pH 3.0 and 7.0, which indicated that La-NM-M41 adsorbent had a greater affinity for the monovalent dihydrogen phosphate. Besides, the dissolution of La from La-natural based under higher acidic conditions was 99.8% [91]. This finding reflected the high toxicity risk of La coated on natural minerals at acidic conditions [46]. Therefore, many works on the development of La-natural-based adsorbent are needed because different La-natural mineral categories may exhibit different stability under acidic conditions. Apart from the influence of solution pH, the coexisting anions such as HCO_3^- and SO_4^{2-} were also affected the adsorption process of phosphate onto La-natural mineral due to the formation of $La_2(CO_3)_3$ from HCO_3^- and ion exchange mechanisms [36,92]. Fig. 6 shows the schematic illustration of the possible interaction mechanism between phosphate and La-natural mineral-based adsorbent.

3.3. La-carbon-based and La-biomass-based adsorbent

Carbon-based materials are regarded as an adsorbent of interest for years among researchers for phosphate removal. The main advantages of carbon-based materials are controllable pore structure and surface chemical properties, facilitating the lanthanum loading. Recently, the uptake capacity of phosphate by lignin-derived porous carbon loaded with $La(OH)_3$ nanorods (LPC@$La(OH)_3$) was augmented from 60.24 to 66.23 and 71.94 mg/g at 25–35 and 45 °C, respectively [23]. The increase of adsorption capacity at elevated temperatures is related to the augmentation of phosphate molecules' movability.

The phosphate sorption capacity by hydroxyl–iron–lanthanum doped activated carbon fiber was also improved as the solution pH adjusted from 2. The maximum capacity appeared at pH 4 [93]. In contrast, the adsorption capacity was decreased with increasing the pH from 4. This finding is linked with the negatively charged and the deprotonation of the La-carbon adsorbent active sites at alkaline pH. Consequently, electrostatic repulsive forces were operative, and the ion exchange was also weakened by the high concentration of OH^- in solution [94]. Such adsorption process is dominated by the Lewis acid-base interaction mechanism, in which the La active site reacts with oxygen anion in the phosphate forming La—O. According to the literature, ligands exchange, electrostatic interactions, and Lewis acid-base interaction are the three main mechanisms for phosphate adsorption on La-carbon based [23,95].

Tang *et al.* found that the solution pH had an insignificant effect on phosphate adsorption onto mesoporous structure La-RHBCs. The main reason is the high stability of encapsulated lanthanum

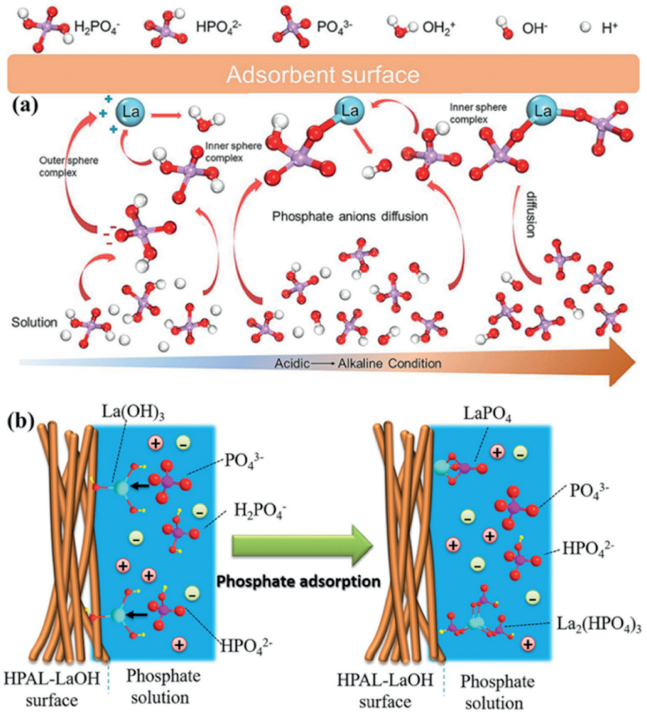

Fig. 6. The possible mechanisms of the removal of phosphate from aqueous solution by La-natural mineral-based adsorbent. (a) phosphate adsorption mechanisms on hydrated lanthanum oxide-modified diatomite. Reproduced with permission [90]. Copyright 2019, Elsevier. (b) Phosphate adsorption mechanisms on calcined nano-porous palygorskite clay matrix with embedded lanthanum hydroxide. Reproduced with permission [81]. Copyright 2018, Elsevier.

hydroxide on the RHBCs through a "shielding effect" [95]. Specifically, majority of La-NMs active sites were anchored on the external surface of host materials because of their micropore structure, whereas La-NPs were both immobilized in the pore channels and to the external surface of the La-NMs. In addition, the uptake of phosphate by La-coated biochar sorbent was hardly interfered by the coexisting anions since the inner-sphere complexes were formed [96]. Fig. 7a represents the adsorption mechanism of phosphate by La-carbon-based adsorbents.

In view of low cost and friendly environmental materials, several La-biomaterials and La-biomass adsorbents have been applied to remove phosphate from water. In recent years, numerous studies are developed various La-biomass adsorbents, such as La-modified pine needles [97], La-modified wheat straw (Ws-N-La) [13], novel La-doped biochars derived from lignocellulosic wastes [57], and La-modified Platanus biochar (La-TC) [30]. The phosphate sorption capacity on lanthanum doped biochars derived from lignocellulosic waste was increased with increasing the temperature due to the fast diffusion of PO_4^{3-} to the adsorption site at high temperature [98]. Moreover, the composite Ws-N-La exhibited a maximum adsorption amount of about 67.1 mg/g. The high adsorption capacity of this La-biomaterial is because of the quaternary ammonium groups on the surface of the wheat straw biomass [13].

At alkaline pH, the sorption capacity of La-biomaterials and biomass adsorbents were inhibited by the release of OH^- from the La-biomaterials [99,100]. Therefore, for this category of La-NMs, the ligand exchange or metal-ligand interaction is one of the major contributors to the adsorption performance [57,99,100]. Fig. 7b illustrates the removal mechanisms of phosphate by La-biomaterial-based adsorbent. The following equations describe the ligand exchange process (Eqs. 4–6):

$$La\text{-}OH + H_2PO_4^- \rightarrow La\text{-}H_2PO_4 + OH^- \quad (2.13 \leq pH \leq 7.20) \tag{4}$$

$$La{=}OH + HPO_4^{2-} \rightarrow La{=}HPO_4 + 2OH^- \quad (7.20 \leq pH \leq 12.33) \tag{5}$$

$$La{\equiv}OH + PO_4^{3-} \rightarrow La{\equiv}PO_4 + 3OH^- \quad (pH > 12.33) \tag{6}$$

3.4. La-polymer and other-based adsorbent

In recent years, more and more research uses polymer as support materials because of its changeable surface properties and high surface activity. Moreover, polymer enhanced the adsorption properties, improved the permeability of phosphate ions, and prevented the adsorbent's aggregation [59]. Currently, several works have produced various La-polymer based adsorbent for phosphate uptake. For example, lanthanum hydroxides modified poly(epichlorohydrin)-ethylenediamine [60]; La hydroxide microcapsules with poly(vinyl chloride) shells [15]; La-Zr binary metal oxide nanoparticles confined in millimeter-sized anion exchanger [101]; nanosized hydrated La(III) oxide confined in crosslinked polystyrene networks [55]; lanthanum-loaded carboxymethyl konjac glucomannan micro-spheres (CMKGM-La) [102] and well-dispersed $La(OH)_3$ nanorods in polyacrylonitrile nanofiber [12]. Lin *et al.* was synthesized lanthanum hydroxide poly (epichlorohydrin)-ethylenediamine composites (PEE@La) [60]. They found that the maximum sorption capacity of PEE@La was 186.57 mg/g. Moreover, PEE@La composite showed notably high pH stability because the matrix (PEE) contained many quaternary ammonium groups, which made the composite positively charged

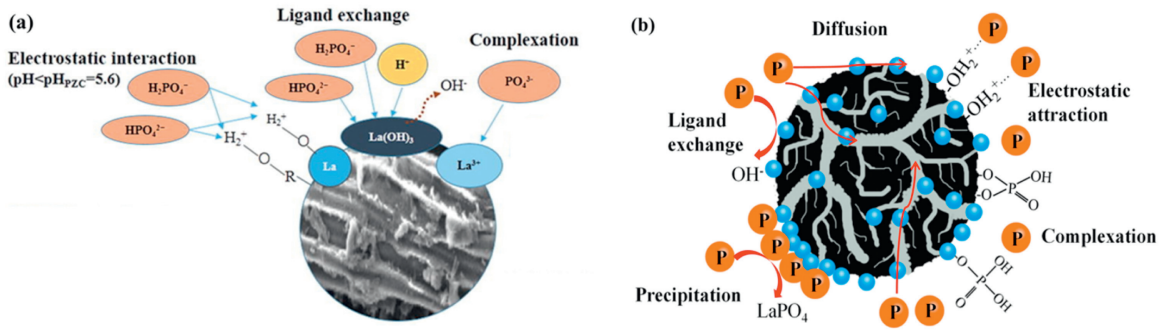

Fig. 7. (a) A schematic diagram describing the possible mechanisms of phosphate onto La-carbon-based. Reproduced with permission [57]. Copyright 2019, Elsevier. (b) The possible mechanisms of phosphate onto La-biomaterial-based adsorbent. Reproduced with permission [95]. Copyright 2019, Elsevier.

in a wide range of pH and effectively sequestrated phosphate ions [60].

The selective adsorption of phosphate by La-polymer-based adsorbents depends on the characteristics of the polymer carrier. Anion exchange resin D201 has been considered as one of the promising polymer supporting media due to its unique properties, such as the high durability, pore spaces, and the uniform dispersion of the La nanoparticles [20]. In addition, anion exchange resin D201 contained tunable networking macropores, covalently bounded positively charged ammonium groups with satisfactory hydraulic properties. Moreover, the charged polystyrene network could also improve La nanoparticles' dispersion inside the carrier and enhance their adsorption activity [55]. Zhang *et al.* reported that the maximum sorption capacity of polymeric anion exchanger supported lanthanum (La-D201) was around 57.4 mg/g at pH 6–7. Furthermore, the adsorption mechanism of phosphate onto La-D201 could explain by the two distinct sites on La-D201, in which the ammonium groups of the host D201 interacting with phosphate *via* electrostatic interaction, and the loaded hydrate lanthanum oxide (HLO) interacting with phosphate through inner-sphere complexation or ligand exchange [56]. Figs. 8a and b summarizes the adsorption mechanisms of phosphate on La-polymer-based.

Apart from the polymer-based support materials, numerous researches have been demonstrated the efficiency of La coated on other host materials. Chen *et al.*, Wang *et al.*, and Yuan *et al.* fabricated lanthanum(III) loaded granular ceramic [26], novel talc encapsulated lanthanum alginate hydrogel [50], and lanthanum hydroxide loaded on molecular sieve [56], respectively. Chen *et al.* observed that phosphate removal efficiency was increased with increasing lanthanum(III) loaded granular ceramic dose, which resulted from the significant amount of the available binding sites on the surface of the adsorbent [26]. Furthermore, Wang *et al.* found that the phosphate removal efficiency was augmented from 30.09% to 92.08% as the adsorbent dosage was added from 0.1 g/L to 1 g/L [37].

Besides, Yuan *et al.* confirmed that phosphate's adsorption capacity on lanthanum hydroxide loaded on molecular sieve (LHMS) had a slight variation in the pH value ranging from 4 to 7. Afterward, the adsorption capacity decreased at pH ranging from 7 to 11. Moreover, fluorine and chloride anions significantly impacted the phosphate removal by LHMS [56]. It resulted from the similar electron cloud distribution between silicate (Si) and phosphate, and the similar molecular structure of the silicate ion and phosphate ion possessing the homologous chemical characteristics [56,103]. The main interaction mechanisms of phosphate on La-other based adsorbent are described in Fig. 8c.

Based on the available literature analysis, the adsorption mechanism of phosphate onto La-other-based adsorbent may involve electrostatic attraction and a surface precipitation process.

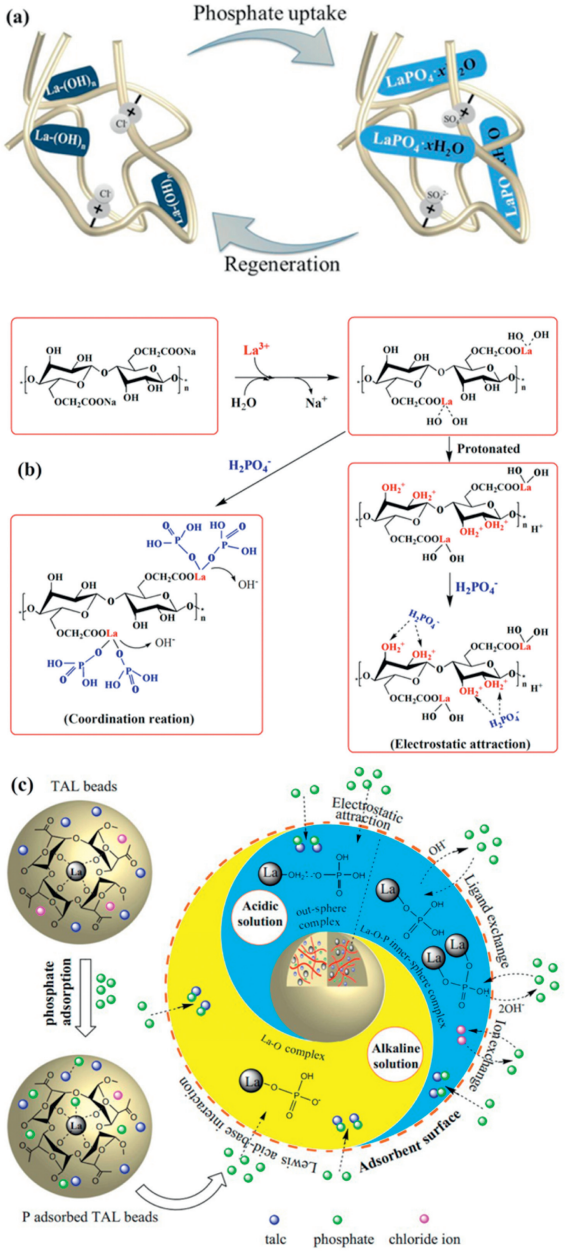

Fig. 8. Schematic of the interaction mechanisms of phosphate with La-polymer based and other based adsorbents. (a) The possible interaction mechanisms between phosphate and nanosized hydrated La(III) oxide confined in crosslinked polystyrene networks. Copied with permission [55]. Copyright 2016, American Chemical Society. (b) The possible interaction mechanisms between phosphate carboxymethyl konjac glucomannan loaded with lanthanum. Copied with permission [102]. Copyright 2018, Elsevier. (c) The possible interaction mechanisms between phosphate and novel talc encapsulated lanthanum alginate hydrogel. Copied with permission [37]. Copyright 2020, Elsevier.

3.5. The possible interaction mechanism between phosphate and La-NMs

The analysis of the interaction mechanism between La-NMs and phosphate is an essential issue to develop an efficient method for producing La-NMs and optimize their efficiency for practical applications. Spectral methods such as FTIR, XRD, and XPS are often used to analyze the interaction mechanisms between phosphate and La-NMs. First, for the single La adsorbent, studies have demonstrated that after adsorption, the appearance of a new band number of 1053 cm^{-1} on the FTIR spectra was observed, corresponding to the P—O asymmetry vibration. This result indicated the chemical adsorption of phosphate onto La surface. Besides, the characteristic peak at 1379 cm^{-1} that was attributed to the vibration of —OH from La—OH was greatly weakened. It would result in the formation of inner-sphere complexation by the exchange of —OH from La—OH with phosphate. Meanwhile, the XPS analysis demonstrated that the formation of new peaks corresponding to the binding energies of 853 and 836.1 eV for La $3d_{3/2}$ and La $3d_{5/2}$, respectively, indicating the formation of La—O—P inner-sphere complexation after ligand exchange [25,39].

Furthermore, numerous research have investigated the possible interaction mechanism between the synthesized La-NMs and phosphate. The XPS spectra analysis of La-NMs after adsorption

showed that the M—O (metal bonded oxide) (at 529.65 eV) was increased. In comparison, the M—OH (metal bonded hydroxide) (at 531.35 eV) was decreased due to the deprotonation of M—OH. This result could explain the ligand exchange between phosphate and hydroxyl functional groups during adsorption [17,70]. The exchange between phosphate and hydroxyl groups from the adsorbent could also be reflected by the high final pH value after the sorption, which indicated that the hydroxide concentration in the solution increased after phosphate adsorption [104].

Moreover, the electrostatic interaction between phosphate and La-NMs was also attributed to the adsorption mechanism. The electrostatic interaction mechanism was depended on the pH_{pzc} of the La-NMs. Number of studies had demonstrated when $pH < pH_{pzc}$, the La-NMs adsorbent surface was positively charged *via* protonation in the form of $M\text{-}OH^{2+}$, which can enhance phosphate adsorption by electrostatic attraction [70]. The possible transformation is shown in the following reaction (Eqs. 7 and 8):

$$LaOH^{2+}/La(OH)_2^+ + H_2PO_4^- \rightarrow La(H_2PO_4)_2^+ + OH^- \quad (7)$$

$$LaOH^{2+}/La(OH)_2^+ + HPO_4^{2-} \rightarrow La(HPO_4)^- + OH^- \quad (8)$$

The competitive adsorption experiments can confirm the formation of inner-sphere complexation or outer-sphere complexation. Recently, Qiu *et al.* found that the sulfate addition can increase in $LaPO_4$ species formation, suggesting the existing SO_4^{2-} can enhance the phosphate adsorption relatively. Such phenomenon for phosphate enhancement further demonstrates the realization of the strong inner-sphere complexation within $LaPO_4$ species [13]. Additionally, Fang *et al.* and Jia *et al.* indicated that the outer-sphere complexation mechanism was usually affected by background ions such as sulfate and bicarbonate in water [28,30].

In summary, there are five major mechanisms (ion exchange, ligand exchange, surface outer-sphere complexation, surface inner-sphere complexation, and electrostatic attraction) that could emphasize the interaction between phosphate and La-NMs. Also, electrostatic attraction and Ligand exchange are always a necessary step for all category of La-NMs. The main reason for the electrostatic attraction is the attraction of negatively charged phosphate ions by the La-NMs positive surface charge ($pH < pH_{pzc}$). Moreover, the ligand exchange and subsequent inner-sphere complexation were related to the phosphate ion forms a covalent chemical bond with a La cation at the adsorbent surface resulting in the release of other potential determining ions such as OH ions previously bonded with the La cation.

4. Desorption and regeneration of La-NMs

It is important to analyze the recovery of La-NMs in laboratory experiments in order to evaluate the potentiality, durability, and stability of La-NMs in eutrophication restoration or in industries. The desorption and re-adsorption analysis are also an essential feature to gain the economic point of view for large-scale [105]. Thus, numerous researchers have studied the regeneration of various La-NMs. Table S3 (Supporting information) summarizes different La-NMs recycle and their re-adsorption efficiency.

The recovery of phosphate from exhausted La-NMs was achieved by using NaOH, NaCl, and HCl solution at a determined time and temperature [18,62]. Xie *et al.* investigated phosphate's desorption from the synthesized lanthanum hydroxide materials and lanthanum oxide adsorbents [18]. Their results showed that phosphate's desorption capacity from lanthanum oxide was deficient, even by increasing the concentration of NaOH to 3 mol/L at 100 °C. This result indicated that the adsorbed $\equiv La\text{-}PO_4$ complex could no longer be easily desorbed by OH^-. Thus, the authors used monazite as desorbent. This method could desorb phosphate from LO by forming insoluble lanthanum hydroxide and soluble Na_3PO_4, which can be easily separated. Phosphate adsorbed on LH could also be recovered in this way. The percentage desorption reached 96.12% for LH [16] and 96.73% for LO [33], respectively. Moreover, the re-adsorption of LH after four cycles still reached 90% [16].

Recently, several studies investigated the regeneration of hybrid metal-based loaded lanthanum such as La@MgAl nanocomposite [49], Mg-La bimetal oxide nanocomposites [44], and La-Zr-Zn ternary oxide [70]. The La-Zr-Zn ternary oxide phosphate-saturated adsorbent regenerated using 0.5 mol/L NaOH solution during 12 h [70]. The authors indicated that the re-uptake of phosphate capacity was decreased due to the irreversible adsorption of phosphate on some La-Zr-Zn active sites. On the other hand, for phosphate saturated Mg/La adsorbent, after four cycles of regeneration, the adsorbent still exhibited a relatively high re-adsorption capacity by 83.07 mg/g [44]. The same author also reported a similar result and indicated that after five adsorption-desorption cycles of La@MgAl adsorbent, the phosphate removal percentage remained over 80% [49]. Banu *et al.* studied the adsorption/desorption of lanthanum(III) encapsulated chitosan-montmorillonite composite using 50 mL of 0.1 mol/L NaOH [106]. Their results showed that the re-adsorption efficiency was retained to 80%, and the adsorption capacities were found to be about 37.9 mg/g even after the fifth cycle.

Moreover, LPC@$La(OH)_3$ could be regenerated in four cycles [23]. Compared to the first recycle, the phosphate removal efficiency was slightly decreased to 93.5% after the second cycle recovery and then to 92.7% after the third regeneration. The study focused on the analysis of the relationship between phosphate-La-NMs binding energy and desorption of phosphate from La-NMs are limited. On the other hand, based on our literature survey, we found that H-bonding interaction such as ligand exchange and inner-sphere complexation are dominated the interaction mechanism of phosphate onto La-NMs. For this reason, the high desorption efficiency of phosphate was obtained from several La-NMs category. This high desorption efficiency might be understood by the relatively weak H-bonding interaction [20].

5. Application to real environmental sample

The available literature reports on the real application of La-NMs to wastewater samples are summarized in Table 1. It is crucial to study the adsorption performance of La-NMs to select and remove phosphate ions from real wastewater in order to evaluate the La-NMs application in wastewater treatment and eutrophication restoration. Chen *et al.* was examined the adsorption capacity of $La(OH)_3$-modified magnetic cobalt ferric nanocomposite toward phosphate in wastewater from Xiang Jiang river (Changsha, China) [17]. The initial phosphate concentration in the water samples was 1.17 mg/L. They demonstrated that the concentration of phosphate was decreased from 1.17 mg/L to 0.05 mg/L within 20 min.

Moreover, Kong *et al.* studied the removal performance of PC@La toward phosphate in sewage wastewater [44]. The initial concentration of phosphate anion in the collected sewage sample was 4.5 mg/L, respectively. They found that a small dose of 1 g/L PC@La could be realized to remove phosphate to less than 0.5 mg/L. Additionally, He *et al.* used La-zeolite (La-Z) to adsorb phosphate in polluted water from the lake [36]. Their finding showed that phosphate concentration in wastewater was reduced from 5.34 mg/L to 0.032 mg/L when 2 g/L of La-Z was added.

Table 1
The adsorption capacity of different category La-NMs in real environmental samples.

Adsorbents	Real sample category	P conc. in wastewater (mg/L)	Adsorbent dosage (g/L)	P-removal efficiency (%) or residual conc. (mg/L)	Ref.
LO-incorporated zeolite	Wastewater	5.34	2	0.32	[36]
MG@La	Polluted water from river Sewage	0.09 0.46	1.25	> 90	[50]
$La(OH)_3/Fe_3O_4$ nanocomposites	Wastewater	1.10	0.10	0.05	[38]
$La(OH)_3$ loaded magnetic mesoporous nanospheres	Polluted water from lake	1.21	0.1–1.0	< 0.05	[103]
Ferrihydrite-coated and lanthanum decorated magnetite	Domestic wastewater	1.70	0.05 - 0.80	0.02	[35]
$La(OH)_3$-$CoFe_2O_4$ nanocomposites	Wastewater from Xiangjiang River	1.17	0.20	97.6 0.05	[17]
La hydroxide loaded on molecular sieve	Wastewater samples from wastewater industry in Shanghai	33	4	< 0.5	[56]
Mesoporous silica films decorated with lanthanum	Water sample from the campus lake	0.51	n.a.	10.60	[85]

n.a.: not available.

6. Conclusion and perspective

In recent years, La-NMs have gained great attention as it has unique functionalities for phosphate removal. Therefore, numerous research in the last ten years focuses on using this category of adsorbents to remove phosphate from synthetic and real wastewater in laboratory scale. Various La-NMs categories such as the single synthesized La hydro(oxide), La-metal based, La-natural mineral-based, La-carbon based, La-biomaterial and biomass-based, La-polymer based were prepared by using the co-precipitation and hydrothermal methods. Moreover, many studies have demonstrated that the synthesis methods have an important role and significant effect on the structure, properties, and adsorption performance of various La-NMs. Tremendous number of research also indicated that La incorporated into the support materials increased the active sites of the synthesized La-NMs. Besides, *pseudo*-second-order and Langmuir models were found to fit the kinetic and isotherm data well. This indicated that the sorption process and behavior of La-NMs were dominated by the chemisorption process and homogeneous monolayer behavior. Current studies have also elucidated that phosphate's adsorption onto La-NMs depended on various experimental conditions such as pH, temperature, sorbent dosage, La content, and the surface properties of La-NMs. Furthermore, many works have shown that the competition of adsorption active sites between OH^- and phosphate ions were dropped the sorption capacity at the alkaline condition. In contrast, at the acidic condition, the adsorption capacity increased due to the ligand exchange mechanism, in which H^+ first attached with La, then attracted the negatively charged phosphate ions. Thus, the uptake of phosphate by La-NMs could be explained by combining different interaction mechanisms such as electrostatic interaction, inner-sphere complexation, and ion exchange *via* Ligand exchange. Furthermore, the saturated La-NMs were successfully recovered using NaOH, HCl, and NaCl as regeneration reagents.

However, based on the present literature surveys, there are still many challenges in the practical application of La-NMs. First, we find that La oxide species could affect the adsorption efficiency La-NMs. Therefore, La hydroxide or carbonate species should successfully synthesize with the carrier materials to achieve favorable phosphate adsorption and desorption. In addition, there are still many works required to improve the irreversible binding of La to the host material because the high durability and stability of La incorporated on the support materials avoid La-NMs dissolution under acidic and alkaline conditions and decrease the risk and toxicity of La-NMs to the environment. Moreover, there is also a strong need for a novel approach to developing the selectivity of La-NMs, even HCO_3^- and F^- introduced in the solution. The application of different category La-NMs to real environmental samples and the recovery of waste should also investigate in-depth in the future.

Furthermore, in order to promote the industrial scale application, profound and comprehensive characterization methods on the surface chemical properties of La-NMs are required to further explain and elucidate the adsorption behaviors and mechanisms. The role and effect of interaction mechanism on La-NMs regeneration should also be explored in-depth in the future. Besides, many research are required to investigate the application of recovered phosphate. Further research should also include the development and application of various La-NMs in large-scale, in order to understand their viability for industrial and environmental clean-up. Finally, we believe that the research gaps mentioned earlier are beneficial to the selection, fabrication, and application of La-NMs for phosphate removal in industry.

Declaration of competing interest

The authors report no declaration of interest.

Acknowledgments

The authors gratefully acknowledge the financial support of the National Natural Science Foundation of China (NSFC) (No. 21876145), Natural Science Foundation (NSF) of Hebei Province (No. B2018203331), and the Support Program for the Top Young Talents of Hebei Province. We also acknowledge the Supporting Plan for 100 Excellent Innovative Talents in Colleges and Universities of Hebei Province (No. SLRC2019041)

Appendix A. Supplementary data

Supplementary material related to this article can be found, in the online version, at doi:https://doi.org/10.1016/j.cclet.2021.01.046.

References

[1] M. Pedro-Monzonís, A. Solera, J. Ferrer, T. Estrela, J. Paredes-Arquiola, J. Hydrol. (Amst) 527 (2015) 482–493.
[2] W. Zhang, Y. Lan, M. Ma, et al., Environ. Int. 142 (2020) 105798.
[3] R. Wang, W. Zhang, L. Zhang, et al., Environ. Sci. Pollut. Res. 26 (2019) 1595–1605.
[4] G. Fink, J. Alcamo, M. Flörke, K. Reder, Global Biogeochem. Cycles 32 (2018) 617–634.
[5] W. Zhang, Y. Tian, Front. Chem. Sci. Eng. 9 (2015) 209–215.
[6] X. Wang, J. Sheng, M. Yang, Chin. Chem. Lett. 30 (2019) 533–540.
[7] S. Zhang, X. Pei, H. Gao, S. Chen, J. Wang, Chin. Chem. Lett. 31 (2020) 1060–1070.

[8] Y. Yang, M. Wu, X. Zhu, et al., Chin. Chem. Lett. 30 (2019) 2065–2088.
[9] M. Zhang, J. Jia, K. Huang, X. Hou, C. Zheng, Chin. Chem. Lett. 29 (2018) 456–460.
[10] X. Pan, J. Ji, N. Zhang, M. Xing, Chin. Chem. Lett. 31 (2020) 1462–1473.
[11] J. Fu, Z. Zhang, G. Li, Chin. Chem. Lett. 30 (2019) 285–291.
[12] J. He, W. Wang, W. Shi, F. Cui, RSC Adv. 6 (2016) 99353–99360.
[13] H. Qiu, C. Liang, J. Yu, et al., Chem. Eng. J. 315 (2017) 345–354.
[14] X. Li, Y. Kuang, J. Chen, D. Wu, J. Colloid Interface Sci. 574 (2020) 197–206.
[15] Y. Makita, A. Sonoda, Y. Sugiura, et al., Sep. Purif. Technol. 241 (2020) 116707.
[16] G. Li, D. Chen, W. Zhao, X. Zhang, J. Environ, Chem. Eng. 3 (2015) 515–522.
[17] Y. Chen, R. Xu, Y. Li, et al., Colloids Surfaces A: Physicochem. Eng. Asp. 599 (2020) 1–11.
[18] J. Xie, Z. Wang, S. Lu, et al., Chem. Eng. J. 254 (2014) 163–170.
[19] D. Copetti, K. Finsterle, L. Marziali, et al., Water Res. 97 (2015) 162–174.
[20] B. Wu, J. Wan, Y. Zhang, B. Pan, I.M.C. Lo, Environ. Sci. Technol. 54 (2020) 50–66.
[21] Y. Zhi, C. Zhang, R. Hjorth, et al., Environ. Int. 145 (2020) 106115.
[22] L. Fang, B. Wu, J.K.M. Chan, I.M.C. Lo, Chemosphere 192 (2018) 209–216.
[23] X. Liu, E. Zong, W. Hu, et al., ACS Sustain. Chem. Eng. 7 (2019) 758–768.
[24] Y. Yang, K. Yuen Koh, R. Li, et al., J. Hazard. Mater. 392 (2020) 121952.
[25] K.Y. Koh, S. Zhang, J. Paul Chen, Chem. Eng. J. 380 (2020) 122153.
[26] N. Chen, C. Feng, Z. Zhang, et al., J. Taiwan Inst. Chem. Eng. 43 (2012) 783–789.
[27] W. Huang, X. Yu, J. Tang, et al., Microporous Mesoporous Mater. 217 (2015) 225–232.
[28] L. Fang, Q. Shi, J. Nguyen, et al., Environ. Sci. Technol. 51 (2017) 12377–12384.
[29] X. Min, X. Wu, P. Shao, et al., Chem. Eng. J. 358 (2019) 321–330.
[30] Z. Jia, W. Zeng, H. Xu, S. Li, Y. Peng, Process Saf. Environ. Prot. 140 (2020) 221–232.
[31] Q. Zhang, Z. Ji, J. Zhou, X. Zhao, X. Lan, Mater. Sci. Forum 724 (2012) 233–236.
[32] Z. Zhong, X. Lu, R. Yan, et al., Sci. Total Environ. 738 (2020) 139636.
[33] J. Xie, Y. Lin, C. Li, D. Wu, H. Kong, Powder Technol. 269 (2015) 351–357.
[34] B. Liu, Y. Yu, Q. Han, et al., Int. J. Biol. Macromol. 157 (2020) 247–258.
[35] H. Fu, Y. Yang, R. Zhu, et al., J. Colloid Interface Sci. 530 (2018) 704–713.
[36] Y. He, H. Lin, Y. Dong, L. Wang, Appl. Surf. Sci. 426 (2017) 995–1004.
[37] B. Wang, W. Zhang, L. Li, et al., Chemosphere 256 (2020) 127124.
[38] B. Wu, L. Fang, J.D. Fortner, X. Guan, I.M.C. Lo, Water Res. 126 (2017) 179–188.
[39] L. Fang, R. Liu, J. Li, et al., Water Res. 130 (2018) 243–254.
[40] S.C. Galbraith, P.A. Schneider, Chem. Eng. J. 240 (2014) 124–132.
[41] Y. Yu, J. Paul Chen, J. Colloid Interface Sci. 445 (2015) 303–311.
[42] X. Xiao, Y. Huang, F. Dong, J. Chem. 2014 (2014) 1–9.
[43] S. Asiri, M. Setkol, S. Guner, et al., Ceram. Int. 44 (2018) 5751–5759.
[44] L. Kong, Y. Tian, Z. Pang, et al., Chem. Eng. J. 382 (2020) 122963.
[45] J. Liu, G. Wang, L. Lu, Y. Guo, L. Yang, RSC Adv. 7 (2017) 40965–40972.
[46] J. Xie, Z. Wang, D. Fang, C. Li, D. Wu, J. Colloid Interface Sci. 423 (2014) 13–19.
[47] T. Liu, X. Chen, X. Wang, S. Zheng, L. Yang, Chem. Eng. J. 335 (2018) 443–449.
[48] H. Hao, Y. Wang, B. Shi, Water Res. 155 (2019) 1–11.
[49] L. Kong, Y. Tian, Z. Pang, et al., Chem. Eng. J. 371 (2019) 893–902.
[50] H. Rashidi Nodeh, H. Sereshti, E. Zamiri Afsharian, N. Nouri, J. Environ. Manage. 197 (2017) 265–274.
[51] K.W. Jung, S.Y. Lee, J.W. Choi, Y.J. Lee, Chem. Eng. J. 369 (2019) 529–541.
[52] S. Dong, Y. Wang, Y. Zhao, X. Zhou, H. Zheng, Water Res. 126 (2017) 433–441.
[53] Y. Zhang, Y. Qian, W. Li, X. Gao, B. Pan, Sci. Total Environ. 683 (2019) 609–616.
[54] J. Xie, L. Lai, L. Lin, et al., J. Environ. Sci. Heal. Part A: Toxic/Hazardous Subst. Environ. Eng. 50 (2015) 1298–1305.
[55] Y. Zhang, B. Pan, C. Shan, X. Gao, Environ. Sci. Technol. 50 (2016) 1447–1454.
[56] L. Yuan, Z. Qiu, Y. Lu, et al., J. Alloys. Compd. 768 (2018) 953–961.
[57] Q. Xu, Z. Chen, Z. Wu, et al., Bioresour. Technol. 289 (2019) 121600.
[58] M. Wang, B. Kong, Y. Zhang, C. Shan, B. Pan, Appl. Surf. Sci. 538 (2021) 147910.
[59] Y. Sun, X. Feng, W. Zheng, J. Chem, Eng. Data 65 (2020) 4512–4522.
[60] L.S. Lin, C.G. Niu, N. Tang, et al., Colloids Surfaces A: Physicochem. Eng. Asp. 588 (2020) 124344.
[61] G. Li, D. Chen, W. Zhao, X. Zhang, J. Environ. Chem. Eng. 3 (2015) 515–522.
[62] J. Xie, Y. Lin, C. Li, D. Wu, H. Kong, Powder Technol. 269 (2015) 351–357.
[63] S. Li, X. Huang, Z. Wan, et al., Chem. Eng. J. 388 (2020) 124373.
[64] Y. Park, C. Gorman, E. Ford, J. Mater. Sci. 55 (2020) 5008–5020.
[65] H. Qiu, S. Zhang, B. Pan, W. Zhang, L. Lv, Chem. Eng. J. 232 (2013) 167–173.
[66] H. Qiu, C. Liang, X. Zhang, et al., ACS Appl. Mater. Interfaces 7 (2015) 20835–20844.
[67] R. Xu, M. Zhang, R.J.G. Mortimer, G. Pan, Environ. Sci. Technol. 51 (2017) 3418–3425.
[68] J. Wang, L. Wu, J. Li, D. Tang, G. Zhang, J. Alloys. Compd. 753 (2018) 422–432.
[69] W. Shi, Y. Fu, W. Jiang, et al., Chem. Eng. J. 357 (2019) 33–44.
[70] T. Wei, G. Zhang, Z. Long, G. Xian, L. Niu, J. Alloys. Compd. 817 (2020) 152745.
[71] L. Wang, J. Wang, W. Yan, C. He, Y. Shi, Chem. Eng. J. 387 (2020) 123305.
[72] J. Lu, H. Liu, X. Zhao, et al., Colloids Surfaces A Physicochem. Eng. Asp. 455 (2014) 11–18.
[73] J. Zhao, J. Liu, N. Li, et al., Chem. Eng. J. 304 (2016) 737–746.
[74] Y. He, H. Lin, Y. Dong, Q. Liu, L. Wang, Chemosphere 164 (2016) 387–395.
[75] W. Shi, Y. Fu, W. Jiang, et al., Chem. Eng. J. 357 (2019) 33–44.
[76] S. Meng, Y. Li, T. Zhang, et al., Water Air Soil Pollut. 224 (2013) 1556.
[77] S. Salehi, M. Hosseinifard, Cellulose 27 (2020) 4637–4664.
[78] X. Li, Q. Xie, S. Chen, et al., Environ. Pollut. 247 (2019) 9–17.
[79] M. Lürling, F. van Oosterhout, Hydrobiologia 710 (2013) 253–263.
[80] M. Lürling, G. Waajen, F. van Oosterhout, Water Res. 54 (2014) 78–88.
[81] L. Kong, Y. Tian, N. Li, et al., Appl. Clay Sci. 162 (2018) 507–517.
[82] B. Ballinger, J. Motuzas, C.R. Miller, S. Smart, J.C. Diniz Da Costa, Sci. Rep. 5 (2015) 8210.
[83] F. Jabeen, D. Hussain, B. Fatima, et al., Anal. Chem. 84 (2012) 10180–10185.
[84] X. Jing, Y. Wang, L. Chen, et al., J. Mol. Liq. 296 (2019) 111815.
[85] X. Jing, Y. Jiang, Y. Wang, et al., Microporous Mesoporous Mater. 296 (2020) 109953.
[86] L. Chen, Y. Li, Y. Sun, Y. Chen, J. Qian, Chem. Eng. J. 360 (2019) 342–348.
[87] M. Mucci, G. Douglas, M. Lürling, Chemosphere 249 (2020) 1–10.
[88] V. Kuroki, G.E. Bosco, P.S. Fadini, et al., J. Hazard. Mater. 274 (2014) 124–131.
[89] G. Li, C. Huo, Y. Li, et al., Int. J. Biol. Macromol. 112 (2018) 1296–1302.
[90] Y. Wu, X. Li, Q. Yang, et al., J. Environ. Manage. 231 (2019) 370–379.
[91] J. Zhang, Z. Shen, W. Shan, Z. Mei, W. Wang, J. Hazard. Mater. 186 (2011) 76–83.
[92] J. Goscianska, M. Ptaszkowska-Koniarz, M. Frankowski, et al., J. Colloid Interface Sci. 513 (2018) 72–81.
[93] J. Liu, L. Wan, L. Zhang, Q. Zhou, J. Colloid Interface Sci. 364 (2011) 490–496.
[94] P. Koilraj, K. Sasaki, Chem. Eng. J. 317 (2017) 1059–1068.
[95] Q. Tang, C. Shi, W. Shi, et al., Sci. Total Environ. 662 (2019) 511–520.
[96] J. Li, B. Li, H. Huang, et al., Sci. Total Environ. 714 (2020) 136839.
[97] X. Wang, Z. Liu, J. Liu, et al., PLoS One 10 (2015) 0142700.
[98] Z. Wang, D. Shen, F. Shen, T. Li, Chemosphere 150 (2016) 1–7.
[99] W. Du, Y. Li, X. Xu, et al., J. Colloid Interface Sci. 533 (2019) 692–699.
[100] T. Liao, T. Li, X. Su, et al., Bioresour. Technol. 263 (2018) 207–213.
[101] Y. Du, X. Wang, G. Nie, L. Xu, Y. Hu, J. Colloid Interface Sci. 580 (2020) 234–244.
[102] X. Zhang, X. Lin, Y. He, et al., Int. J. Biol. Macromol. 119 (2018) 105–115.
[103] J. Yang, L. Zhou, J. Zhang, et al., Chem. Eur. J. 19 (2013) 5578–5585.
[104] Q. Zhang, Q. Du, T. Jiao, et al., Chem. Eng. J. 221 (2013) 315–321.
[105] Y. Song, P. Yuan, P. Du, et al., Appl. Clay Sci. 186 (2020) 105450.
[106] H. Thagira Banu, P. Karthikeyan, S. Meenakshi, Int. J. Biol. Macromol. 112 (2018) 284–293.